Ultrathin Ge epilayers on Si produced by low-temperature PECVD acting as virtual substrates for III-V / c-Si tandem solar cells

Monalisa Ghosh, Pavel Bulkin, François Silva, Erik Johnson, Ileana Florea, Daniel Funes-Hernando, Alexandre Tanguy, Charles Renard, Nicolas Vaissiere, Jean Decobert, et al.

Solar Energy Materials and Solar Cells xxx (xxxx) 111535

Contents lists available at ScienceDirect

Solar Energy Materials and Solar Cells

journal homepage: www.elsevier.com/locate/solmat

Ultrathin Ge epilayers on Si produced by low-temperature PECVD acting as virtual substrates for III-V / c-Si tandem solar cells

Monalisa Ghosh [a], Pavel Bulkin [a], François Silva [a], Erik Johnson [a], Ileana Florea [a], Daniel Funes-Hernando [a], Alexandre Tanguy [b], Charles Renard [c], Nicolas Vaissiere [d], Jean Decobert [d], Iván García [e], Ignacio Rey-Stolle [e], Pere Roca i Cabarrocas [a, *]

[a] Laboratoire de Physique des Interfaces et des Couches Minces (LPICM), CNRS, Ecole Polytechnique, Institut Polytechnique de Paris, 91128 Palaiseau, France
[b] Laboratoire de Mécanique des Solides (LMS), Ecole Polytechnique, Institut Polytechnique de Paris, 91128 Palaiseau, France
[c] Centre de Nanosciences et de Nanotechnologies (C2N), 10 Boulevard Thomas Gobert, 91120 Palaiseau, France
[d] III-V Lab, 1 Avenue Augustin Fresnel, 91767, Palaiseau Cedex, France
[e] Instituto de Energía Solar, Universidad Politécnica de Madrid, Avenida Complutense, 30, 28040 Madrid, Spain

ARTICLE INFO

Keywords:
Virtual substrate
Germanium heteroepitaxy
III-V on Silicon
Low-temperature PECVD
Tandem solar cells

ABSTRACT

Ultrathin (20 nm) epitaxial films of germanium are deposited on crystalline silicon wafers, to act as virtual substrates for the growth of III-V materials, opening a low-cost approach to tandem solar cells. Such ultrathin layers allow for material cost reduction, along with the possibility of using the silicon wafer as the bottom cell in tandem devices. A simple plasma-enhanced chemical vapor deposition (PECVD) process at 175 °C has been optimized to deposit these heteroepitaxial germanium films, which grow directly on the silicon wafers without any intermediate silicon-germanium alloy. Thanks to an *in-situ* plasma cleaning step prior to Ge epitaxy, the films can sustain high-temperature annealing in vacuum (up to 800 °C) without any delamination. The suitability of the germanium heteroepitaxial films as virtual substrates is analyzed by depositing III-V layers on them by conventional growth methods like chemical beam epitaxy (CBE) and metalorganic chemical vapor deposition (MOCVD). The properties of the GaAs films deposited on the virtual substrates are comparable in terms of roughness, microstructure, and crystallinity to these of the III-V layers co-deposited on c-Ge wafers, pointing at the effectiveness of the ultrathin c-Ge epitaxial layers to act as virtual substrates for III-V epitaxial growth. Moreover, growing the c-Ge layers on c-Si substrates with 5° miscut avoids the formation of antiphase domains. These substrates are finally used to demonstrate proof of concept tandem solar cells, proving the suitability of our low temperature and ultrathin virtual substrate approach.

Credit section

Daniel Funes-Hernando: Investigation

1. Introduction

The lattice parameter of germanium almost perfectly matches that of gallium arsenide which makes it a suitable substrate for epitaxial growth of GaAs [1,2]. The III-V materials-based multijunction solar cells, though holding the record conversion efficiency values [3], are expensive due to the high cost of substrates as well as of the deposition process, which limits the use of these cells for terrestrial applications. The major cost of these cells comes from the use of monocrystalline semiconductor wafers like GaAs or Ge as substrates for epitaxial growth of the III-V layers. One major direction of thought is lifting off the solar cell stack from the substrate and reusing the wafers [4,5]. Another approach to solving the issue is replacing the crystalline germanium wafer as the substrate for III-V epitaxy with a germanium thin film deposited on a silicon wafer (the 'virtual substrate'). This shall drastically reduce the cost of GaAs cells as the price of monocrystalline GaAs or Ge wafer is about 100–130 $ for a 6-inch wafer, while solar-grade c-Si wafer of the same size is about 0.5$ [6]. The lower cost of silicon wafers originates from the higher abundance of silicon in the earth's crust than germanium, the higher mechanical strength of c-Si, and the well-established processing technology of the silicon industry [6–11].

* Corresponding author.
E-mail address: pere.roca@polytechnique.edu (P. Roca i Cabarrocas).

https://doi.org/10.1016/j.solmat.2021.111535
Received 31 July 2021; Received in revised form 25 November 2021; Accepted 1 December 2021
0927-0248/

That being said the epitaxial growth of germanium films on c-Si has its challenges. The main reason for the challenges in the heteroepitaxy of germanium on silicon being the 4.18% mismatch between their lattice parameters. Consequently, germanium films deposited on silicon wafers generally have high threading dislocation densities (TDD ~ 10^5-10^7 cm^{-2}) [12]. Many solutions have been tried to solve these issues. One of them is growing a buffer layer (10 nm to a few microns) of silicon-germanium (Si_xGe_{1-x}) at the interface between the silicon wafer and a germanium thin film [13]. The fully relaxed Si_xGe_{1-x} acts as a template to match the lattice constant of silicon with that of germanium and thereby ensures a low defect density epitaxial growth [13–16]. A second approach is the growing of two layers of germanium, in which the first germanium layer is obtained at a lower temperature (300 °C–400 °C) on the silicon, leading to a relaxed crystallographic structure. This first layer will in turn act as the base for the growth of a high temperature (600 °C–700 °C) and higher quality germanium layer [17–23]. Another less conventional way has been studied by some groups, which is known as selective area deposition. In this method, the material can grow only on selective unmasked areas and the dislocations glide from the edge of patterns in which the germanium film has grown [24–28]. Micron-thick germanium films deposited on c-Si wafers have also been used as virtual substrates for III-V deposition by various groups [8–11,29–31]. A 2-μm thick Ge film was deposited on (100) silicon with 6° miscut along the [110] direction at a temperature of 650 °C by metalorganic chemical vapor deposition (MOCVD) process by Wang et al. [8] and was used to grow single-junction GaAs solar cell. Kim et al. deposited a 1-μm thick Ge layer on (100) silicon also by MOCVD at 850 °C which was used to make GaInP solar cells and showed that the germanium virtual substrate works as well as a conventional germanium substrate [9]. A 3–5 μm thick germanium layer grown by reduced pressure chemical vapor deposition (RP CVD) at 900 °C on a silicon wafer used as the virtual substrate for making the triple-junction solar cells, allowed Garcia et al. to demonstrate that this strategy produces devices with performances approaching those of using germanium wafers as substrates [10,11].

Previous works done in our laboratory have demonstrated that instead of going for the aforementioned two-step processes or high deposition temperature, the germanium thin films can be grown epitaxially on silicon wafers using plasma-enhanced chemical vapor deposition (PECVD) at a low temperature of 175 °C [32,33]. This has been made possible by adopting the process conditions under which positively charged clusters contribute to the growth of the film. Acceleration of the clusters by the sheath potential gives them high enough energy to produce a temperature spike upon impact on the substrate resulting in their melting [34]. Under these conditions, even though the average substrate temperature remains low (175 °C), locally (at the nanometer scale) the temperature can be higher than the melting point of the clusters and thus result in a local melting and epitaxial growth [35].

Based on the insights gained from our previous works [32,33] and the ability to grow ultrathin (20 nm) epitaxial Ge films at a low substrate temperature using a single-step PECVD process without any interfacial layer, in the present work we intend to optimize and assess the performance of ultrathin germanium epitaxial films as virtual substrates for the growth III-V materials. Detailed structural studies of the GaAs thin film grown on our virtual substrates are carried out using a wide range of techniques. The motivations for going for such ultrathin layers (20 nm) are to reduce material costs, to cut down on the optical losses in the germanium layer and also to be below the critical thickness for crack propagation due to thermal mismatch between Ge and Si [36,37]. As a proof of concept, we demonstrate a tandem solar cell where the c-Si substrate acts as the bottom cell, while the III-V top cell has been directly grown by MOCVD on the Ge|Si virtual substrate.

2. Experimental methods

Fig. 1 summarizes the process flow for the fabrication of a tandem solar cells starting from a c-Si wafer. The germanium thin films, which will be used as virtual substrates for III-V deposition, are deposited using a standard capacitively coupled radio frequency (13.56 MHz) reactor by plasma-enhanced chemical vapor deposition (PECVD) at a temperature of 175 °C [38]. 4-inch polished n-type crystalline (100) silicon wafers without miscut, thickness 280 μm, resistivity 1-5 Ohm-cm from TopSil, have been used as the substrates for germanium deposition if not stated otherwise. The native oxide layer on the wafers is removed by dipping them for 30 s in dilute hydrofluoric acid (5% HF in deionized water). The substrates are quickly transferred to the reactor which is pumped down to a base pressure below $5x10^{-7}$ mbar. Prior to the deposition process, a SiF_4–H_2 plasma treatment (20 sccm – 300 sccm, 100 mTorr, 5 W for 30 s) is applied on the wafers to remove any trace of ambient contamination, in particular water absorption and surface oxidation [39,40]. Germane (GeH_4, 1% in hydrogen, H_2) and hydrogen (H_2) were used for the epi-PECVD process.

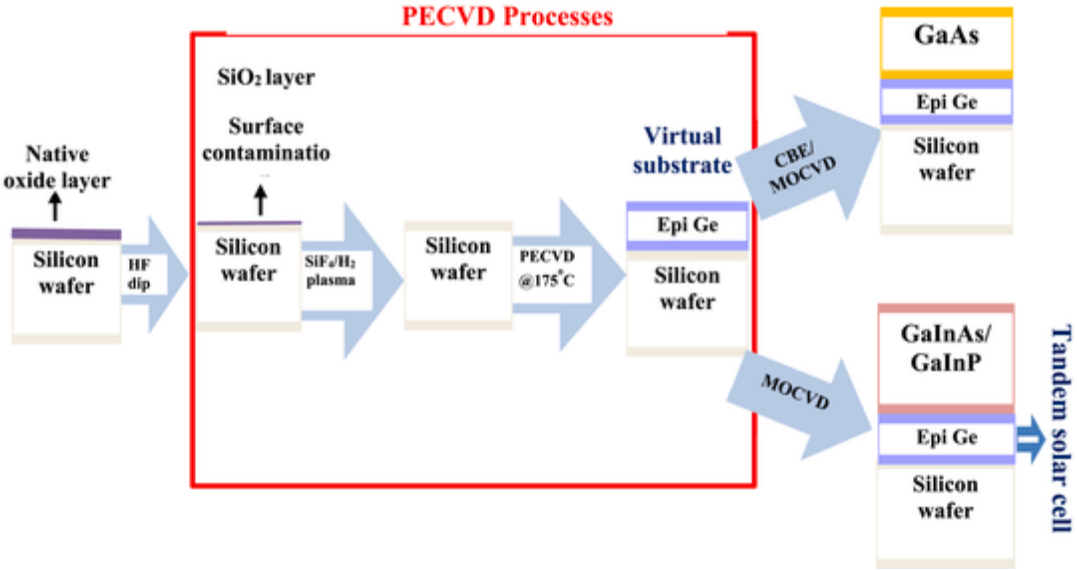

Fig. 1. Schematic illustration of the experimental process flow for the production of virtual (epi Ge/c-Si) substrates and their application for the growth of GaAs layers and tandem solar cells.

As shown in Fig. 1, GaAs thin films are deposited via two different routes to test the compatibility of the as-deposited germanium films to act as a virtual substrate for the growth of III-V films. The first route is carried out in a chemical beam epitaxy (CBE) system with a base pressure of 1.5×10^{-7} mTorr [41], by which GaAs films are grown on the virtual substrate. In this process, the germanium thin films are annealed under a vacuum up to 650 °C to remove their surface oxide, which is *in-situ* monitored with RHEED (Reflection High Energy Electron Diffraction) analysis. GaAs is then deposited for 5 min at 600 °C using trimethylgallium (TMGa) and tertiarybutylarsine (TBAs) as gas precursors without any carrier gas. The V/III ratio of [TBAs]/[TMGa] is kept at 10 while maintaining a pressure of 49.5 mTorr in the growth chamber.

In the second route, GaAs is epitaxially grown using the MOCVD process on Ge|Si virtual substrate. An AIXTRON Close-Coupled Showerhead reactor with trimethylgallium (TMGa) and arsine (AsH_3) are the source materials mixed with hydrogen (H_2) as a carrier gas at a temperature of 680 °C is used for the MOCVD process. The growth rate of the GaAs layers is determined using an in-situ Laytec EpiCurve TT tool based on laser reflectometry operating at a wavelength of 980 nm. Last but not least, GaInP/GaInAs layers and solar cells are deposited using MOCVD in a horizontal, low-pressure, research-scale AIX200/4 reactor at a temperature of 670 °C using TMGa, TMIn, TMAl, AsH_3, PH_3, DMZn, CBr_4, DTBSi, and DETe as precursor source gases. The performance of these III-V layers in a solar cell is further analyzed by fabricating a tandem solar cell with the silicon wafer of the virtual substrate used as the bottom cell. Standard photolithography and wet etching processes are used for making the devices. The back contact of the devices consists of a Pd/Ti/Pd/Al layer stack, which allows sintering at low temperatures, while the front contact is made of electroplated gold. The solar cell devices are 0.1 cm^2 in area and no antireflection coating (ARC) has been applied. Further processing details have been published elsewhere [11,36].

The optical and structural properties of the germanium thin films, as well as the GaAs layers deposited on top of them, are characterized using a wide variety of techniques: spectroscopic ellipsometry (Horiba Jobin-Yvon), optical microscopy (Leica Microsystems DM2700 M), hydrogen exodiffusion, Raman spectroscopy (Horiba Jobin Yvon), and X-Ray diffraction (D8 Discover Bruker). Electron microscopy-based techniques such as electron backscattered diffraction (EBSD) (Symmetry camera with AZTEC acquisition software–provided by Oxford Instruments) and scanning electron microscopy (Hitachi S-4800 and QUANTA 650 FEG-ESEM), and transmission electron microscopy (Titan-Themis electron microscope) are used to characterize the information regarding the homogeneity of the films and their crystalline quality. Moreover, energy dispersive x-ray spectroscopy (EDX) analysis has been performed to determine the chemical composition at the c-Si/Ge/GaAs interface. Finally, external quantum efficiency (EQE) and J-V characteristics of the tandem c-Si/III-V solar cells are also measured. External quantum efficiency (EQE) is analyzed by a custom-build setup based on a Xe lamp and a monochromator and using the lock-in technique for signal detection and an extra detector for monitoring fluctuations in the irradiance. Current density-voltage (J-V) curves under illumination are taken using a Xe-lamp-based solar simulator and a Keithley current-voltage source/monitor unit. The light spectrum and irradiance used are not precisely calibrated but are close to 1-sun AM1.5G solar spectrum.

3. Results and discussions

3.1. Germanium virtual substrate

From the experience gained in the previous studies in our laboratory, it is understood that a SiF_4/H_2 plasma pre-treatment of the crystalline silicon wafers, before PECVD, improves the quality of the epitaxial films as it removes surface contamination and can etch out any silicon oxide which may be formed during the time delay between the HF treatment of the silicon substrates and loading them within the PECVD chamber [39,40]. Fig. 2(a) shows the imaginary part of the pseudo-dielectric function of Ge layers grown on c-Si for two samples, one grown on the HF treated substate and the other with the same HF dip, followed by a SiF_4/H_2 plasma treatment (20 sccm 300 sccm), at a pressure of 0.5 Torr for 30 s. One can see that the SiF_4/H_2 plasma clearly improves the crystallinity of the material as shown by the higher amplitude of the imaginary part of the pseudo-dielectric function (for photon energies above 2.2 eV) with respect to that of the sample without SiF_4/H_2 plasma treatment. The modelling of the experimental data for the sample treated with a SiF_4/H_2 plasma using the layer stack shown in the inset, indicates that the film is fully crystallized (100% c-Ge), with a thickness of 54.7 nm. Moreover, the model indicates that the c-Ge film has an abrupt interface with the c-Si substrate, and a 1.8 nm surface roughness, described as a mixture of 12% c-Ge and 88% GeO_2, most likely due to the oxidation of the sample after its deposition and exposure to ambient air. Thus, it has been henceforth decided to use a SiF_4/H_2 plasma pre-treatment for all the samples before PECVD of germanium.

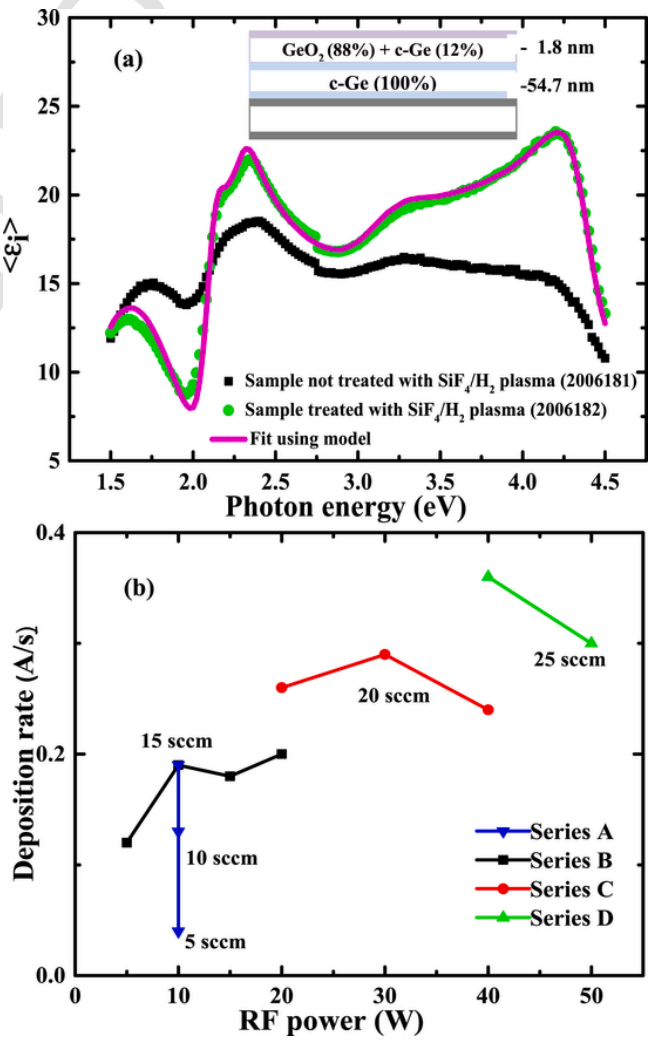

Fig. 2. (a) Imaginary part of the pseudo-dielectric function as deduced from ellipsometry measurements for two films obtained with and without SiF_4/H_2 plasma pre-treatment (inset shows the layers as fitted via model) (b) Effect of RF power on the deposition rate of epitaxial germanium thin films for different values of the GeH_4 flow rate.

To find the optimum window for the growth of epitaxial germanium, various sets of samples were deposited using germane (1% in hydrogen) flow rates ranging from 5 sccm to 25 sccm and RF power for the PECVD process ranging from 5 W to 50 W as shown in Table 1. The hydrogen flow rate and total gas pressure during deposition are kept constant at 500 sccm and 1.7 Torr respectively while the distance between the electrodes was maintained at 22 mm. All samples are analyzed by optical microscopy to check the quality of the film's surface and by ellipsometry to find the thickness, obtain the deposition rate, and crystallinity of the layers. The germanium films are uniform/featureless by the appearance to the naked eye and under a microscope and are highly reflective. Table 1 shows the process conditions and growth rate obtained for four series of samples, for which we are aiming at increasing the deposition rate while keeping a good crystalline quality as determined from the modeling of the ellipsometry spectra of the films. For the A series, the GeH_4 flow rate is increased from 5 sccm to 15 sccm under a constant RF power of 10 W. As shown in Fig. 2(b) the deposition rate increases with GeH_4 flow rate suggesting that for these process conditions the GeH_4 is depleted. For the samples labeled as series B, deposited with a constant GeH_4 flow rate of 15 sccm, we can observe an increase in deposition rate when the RF power is increased from 5 to 10 W and it saturates at 15 and 20W, again supporting the hypothesis that the deposition rate is controlled by the GeH_4 flow rate (note that GeH_4 is diluted to 1% in H_2). Finally, for series C and D the GeH_4 flow rate is increased up to 20 and 25 sccm respectively. We can observe a decrease in the deposition rate at the higher power for both the series, again indicating GeH_4 depletion as well as the etching of the growing film by the excess of atomic hydrogen in the plasma. From the above optimization process, it is found that all the samples are comparable as they all have ellipsometric curves similar to that of sample 2006182 (green triangles) shown in Fig. 2(a). In the following sections, the process conditions are fixed at RF power 10 W and GeH_4 flow rate 10 sccm, obtaining a reasonable deposition rate while avoiding excessive ion bombardment at higher RF power which could increase the strain in the thin films.

Table 1
Effect of GeH4 flow rate (2% GeH_4 in H_2) and RF power on the deposition rate of four series of epitaxial germanium films deposited on (100) c-Si substrates at 175 °C. The total pressure is kept constant at 1700 mTorr.

Series	Germane flow rate (sccm)	RF power (W)	Growth rate Å/s	Sample name
A	5	10	0.04	1911181
	10	10	0.13	1911182
	15	10	0.19	1911183
B	15	5	0.12	1911191
	15	10	0.19	1911183
	15	15	0.18	1911192
	15	20	0.20	1911193
C	20	20	0.26	1912163
	20	30	0.29	1912164
	20	40	0.24	1912181
D	25	40	0.36	1912182
	25	50	0.30	1912183

Fig. 3 (a) shows the imaginary part of the pseudo-dielectric function of an optimized c-Ge thin film deposited on a c-Si substrate, compared to that of a reference c-Ge wafer. A nearly perfect match is observed in the energy range from 2 to 3 eV, indicating that the deposited layer is indeed c-Ge. By fitting the ellipsometry spectra using Deltapsi2 software, we found that a thin layer of germanium oxide (about 1.7 nm) has formed on the germanium film (thickness

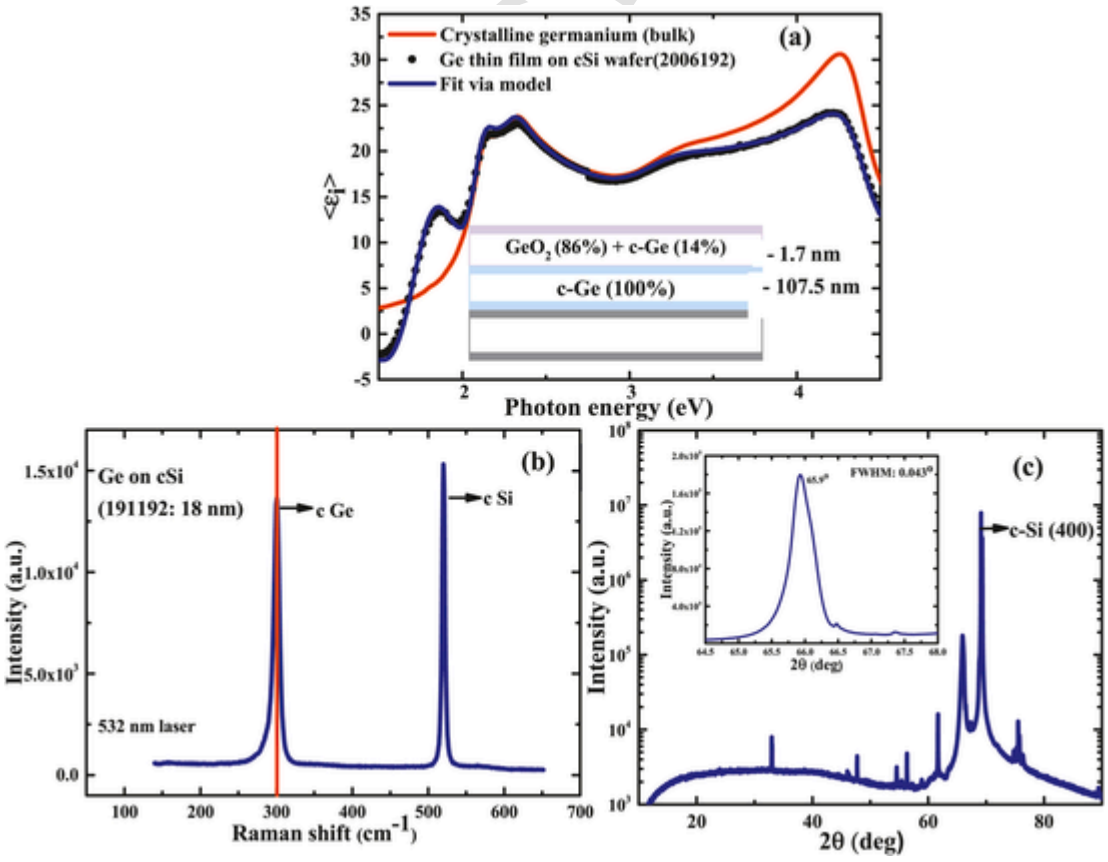

Fig. 3. (a) Imaginary part of the pseudo-dielectric function of the germanium film deposited on silicon when compared with that of crystalline germanium (inset shows the layers as fitted via model) (b) Raman spectra of Ge on cSi (100) substrate (c) XRD pattern of a Ge film deposited on a silicon wafer (the inset shows a magnified (004) Ge peak). (For interpretation of the references to colour in this figure legend, the reader is referred to the Web version of this article.)

107 nm), which has grown directly on the silicon wafer without forming any interfacial mixed germanium-silicon layer. The germanium oxide on the surface is most probably formed due to oxidation of the film upon exposure to the atmosphere when the film has been taken out of the deposition chamber for ex-situ ellipsometry analysis. The difference at low energy (1.5–2 eV) between the spectrum of the bulk c-Ge and that of the virtual substrate is due to interference fringes forming as a result of the difference in refractive index between the c-Ge thin film and the c-Si wafer.

The structure of the sample has been further analyzed at room temperature using Raman spectroscopy at an excitation wavelength of 532 nm. The Raman spectra of a germanium film (sample 191192, ~18 nm thick) deposited on silicon shown in Fig. 3(b) displays a sharp characteristic peak of crystalline germanium at 300 cm^{-1} from Ge–Ge TO phonon mode, along with the characteristic peak of TO phonon mode of the c-Si substrate at 520 cm^{-1}. The characteristic peak for Si–Ge phonon mode generally observed at 400 cm^{-1} is not present in our spectra. This points out the epitaxial growth of the germanium films on the silicon substrate and the most probable lack of Si–Ge mixing at the interface [30,42,43]. Fig. 3(c) shows the X-ray diffraction pattern of the as-deposited germanium thin film with an inset showing XRD profile in the vicinity of (400) peak of germanium at 65.9°. The (400) peak position of the as-deposited film matches that of the bulk reference Ge (400) peak (Ref JCPDS pattern: 00-004-0545). The germanium peak is quite symmetric and does not have any broadening while moving towards higher incidence angles indicating that there is no intermixing of germanium and silicon at the interface (confirmed by STEM-HAADF EDX analysis presented in section 3.2.2). Also, the shift of peak position towards higher or lower values will mostly point at a tensile or compressive strain in the crystal [13,18,21], which is not the case here. Thus, from the structural characterizations done on the as-deposited samples, it can be inferred that dense germanium films without any interfacial silicon-germanium layer can be directly deposited on c-Si by PECVD at 175 °C. The films grow epitaxially with the same orientation as the (100) crystalline silicon wafer and have a small surface roughness, of the order of 1.7 nm as shown in the inset in Fig. 3 (a).

For the germanium films to act as a virtual substrate for GaAs growth, they must sustain the conditions of the III-V deposition process, i.e. neither suffer from blistering nor from delamination. At present, III-V layers are mostly grown by processes like molecular beam epitaxy (MBE), chemical beam epitaxy (CBE), and metalorganic chemical vapor deposition (MOCVD) [44,45]. These deposition processes take place at a high temperature of at least 500 °C, while in the present work the germanium films are grown at a temperature of 175 °C. To check the behavior of the films at high temperatures, they were annealed in vacuum up to 800 °C. The exodiffusion of hydrogen from the material is monitored using a quadrupole mass spectrometer. Fig. 4(a) shows the hydrogen desorption spectra as a function of temperature as the germanium films (2006192: thickness 110 nm) are heated at a ramp of 10 °C/min up to 800 °C. The negligible amount of hydrogen coming out of the samples points to a lack of hydrogen incorporation in the films and supports the hypothesis of a dense and highly crystallized germanium epitaxial film. Moreover, this annealing has not resulted in any visible peel-off or any change in the surface appearance of the films, also confirmed by the optical microscopy image shown in Fig. 4(b). The surface of the germanium films is smooth, without any features both before and after annealing. Fig. 4(c) shows an optical microscope image of a c-Ge film deposited on a c-Si wafer that has not been submitted to the SiF_4/H_2 plasma before c-Ge epitaxy (Sample 2006181). In this case, a large number of defects and blisters appear on the surface of the sample annealed at 800 °C, revealing the positive effect of SiF_4/H_2 plasma pretreatment of silicon wafers before germanium epitaxy. Therefore, the

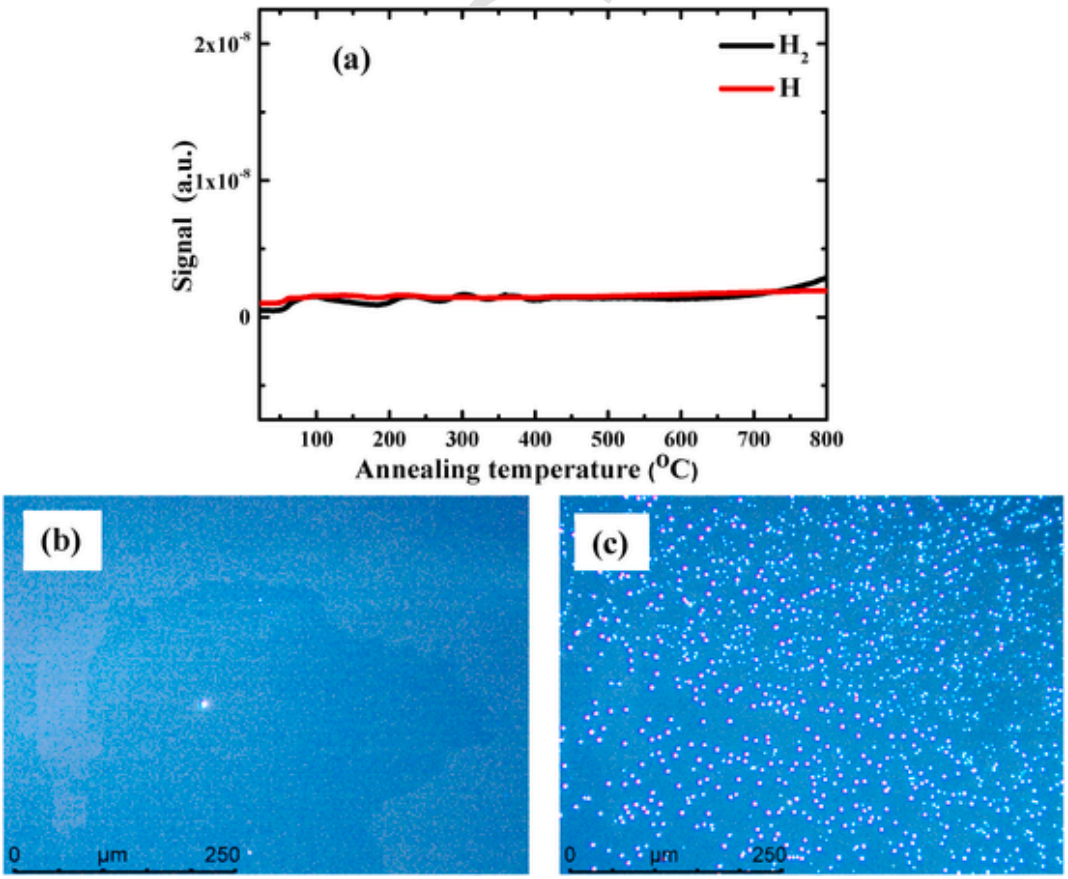

Fig. 4. (a) Hydrogen exodiffusion for the Germanium film (2006192) upon annealing at 800 °C in vacuum. Optical microscopy image after annealing at 500 °C for (b) 2006192-sample which is in-situ SiF_4/H_2 plasma treated before Ge epitaxy and (c) 2006181 -sample not treated with *in situ* SiF_4/H_2 plasma before Ge deposition.

SiF_4–H_2 plasma cleaning step combined with the optimized epitaxial Ge conditions result in excellent c-Ge films which are not affected by the high temperature annealing and take us a step further towards establishing their suitability as 'virtual substrates' for III-Vs growth.

3.2. Deposition of III-V layers on Ge virtual substrates

3.2.1. GaAs by CBE

The CBE method [40] has been used to deposit GaAs thin films on the as-deposited germanium virtual substrates (~20 nm thick Ge film on (100) c-Si wafer without miscut). The deoxidation of the Ge|Si surface is monitored by RHEED. The Ge virtual substrates are annealed under vacuum in the deposition chamber up to 650 °C (for 10 min) to remove the germanium oxide which inevitably grows during the transfer of the germanium thin film from the PECVD set-up to the CBE system. A clear 2x1 Ge reconstruction is observed from 450 °C and becomes more and more streaky until 650 °C, indicating a complete deoxidation of the surface. After verification of the fact that the surface is clean of germanium oxide, the temperature is lowered to 600 °C and the deposition process of gallium arsenide is initiated. The first step consisted of introducing solely TBAs (for 2 min) under a total pressure of 9.9 mTorr. In the second step, TMGa is introduced, and the total pressure is increased to 49.5 mTorr achieving a V/III ratio of [TBAs]/[TMGa] = 10. The GaAs growth is performed for a duration of 5 min.

After GaAs deposition, the samples are analyzed using optical microscopy. The surface of the gallium arsenide film appears rough under an optical microscope and has a milky white appearance. The SEM micrographs also reveal a very rough surface morphology with the presence of antiphase domains and defects as shown in Fig. 5(a). Fig. 5(b) shows the XRD pattern for the as-deposited gallium arsenide sample, displaying a strong peak at 66.1° which coincides with the (400) peak of bulk GaAs, in addition to the c-Si substrate peak at 69.1°. These results show that GaAs can be indeed deposited on the virtual substrate; however, the quality of the gallium arsenide films with respect to surface roughness and presence of defects has to be improved.

3.2.2. GaAs by MOCVD

MOCVD, another standard technique to grow III-V materials, has also been applied to study the suitability of our Ge/Si virtual substrates for the growth of GaAs. In this case, using optimized conditions for homoepitaxial growth of GaAs at 680 °C, 350 nm-thick GaAs layers were simultaneously grown on both a reference (100) germanium wafer as well as on our virtual substrate (~20 nm thin Ge film on (100) cSi wafer with no miscut). Under the optical microscope, it is observed that both GaAs films have similar roughness and surface features as shown in Fig. 6(a) and (b). Ellipsometry measurements carried out on both samples (not shown) feature the same pattern with peaks of the same intensity at higher energies, which points to the similar roughness of the GaAs samples deposited on both a c-Ge wafer and our germanium virtual substrate. The SEM images of both samples, shown in Fig. 6(c) and (d), reveal the presence of antiphase domains, similar to what is observed in the case of the CBE growth. Thus, these antiphase domains are not related to the quality of our Ge virtual substrate but to the use of (100) exactly oriented (flat) wafers. As a matter of fact, antiphase domains are common in GaAs growth on flat wafers, but this can be reduced by the use of miscut wafers. This led us to shift the germanium growth process to a silicon wafer with a miscut of 5° towards <110> (2-inch single side polished, thickness 500 μm, p-type, resistivity 1-10 Ohm-cm, from Silicon Materials). The epi-PECVD Ge films are observed to grow with the same deposition rate and to have the same material properties on the c-Si wafer with 5° miscut as for the previous flat c-Si substrates. In this case (5° miscut wafer), it is observed that the GaAs films grown on the virtual substrates are smoother and do not have anti-phase domains when observed under SEM as shown in Fig. 7(b). On the contrary, the same deposition on a virtual substrate based on an exactly oriented (100) c-Si wafer displayed antiphase domains as shown in Fig. 7(a). The lack of antiphase domains when using a 5° miscut wafer points to the fact that the germanium thin film on the miscut wafer must preserve the misorientation of the silicon substrate, which is an important factor for eligibility of the germanium epitaxial layer to act as a virtual substrate.

To compare further the crystalline quality of the GaAs films, samples were co-deposited on germanium virtual substrates on (100) exactly oriented silicon wafers (type A) and on silicon wafers with a 5° miscut towards (100) (Type B). The properties of both samples were characterized by electron backscattering diffraction (EBSD) and transmission electron microscopy (TEM). Fig. 7 (c) and 7 (d) show the EBSD results for both types of films. A very low value of surface misorientation (< 0.25°) is observed at the surface for both films. Nevertheless, the statistical distribution of the local misorientation values from EBSD given in the insets of Fig. 7 (c) and 7 (d) shows that the misorientation is lower (< 0.1°) for the sample of type B than for the sample of type A. Such low numbers for misorientation point at the monocrystalline nature of the film and to the lack of grain boundaries on the gallium arsenide surface.

To obtain a better insight on the quality of the epitaxial GaAs films and on the defects at the interface we carried out High-Resolution STEM-HAADF observation on the cross-section lamellas corresponding to layers grown on both types of substrates: exactly oriented (100) c-Si (type A) and (100) c-Si with a 5° miscut towards <110> (type B). The cross-section lamellas for TEM observation have been prepared using a standard lift-out procedure within a Focused Ion Beam dual-beam microscope (FIB, FEI-Scios DualBeam). Fig. 8(a) and (b) show low magni-

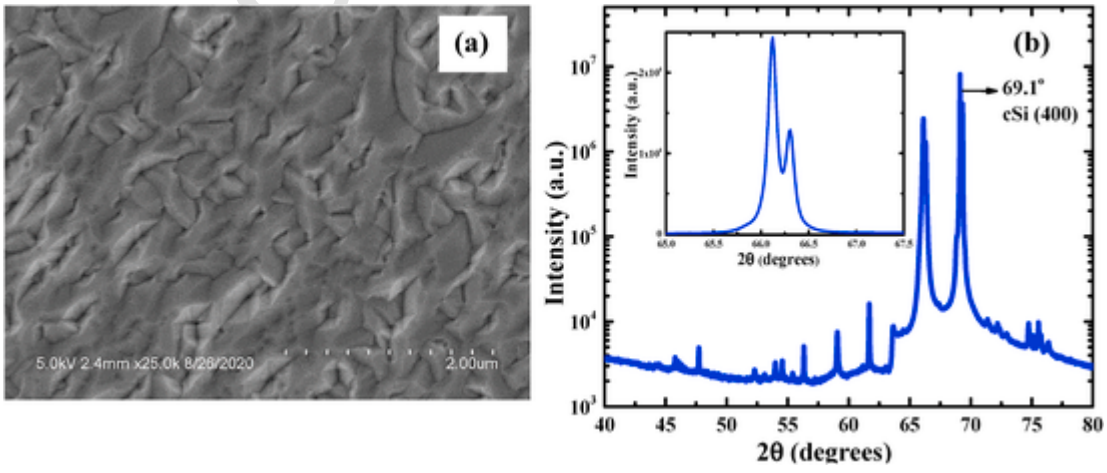

Fig. 5. (a) Scanning electron microscopy image, (b) X-ray diffraction pattern of GaAs films grown on a virtual substrate by CBE (inset showing GaAs peak).

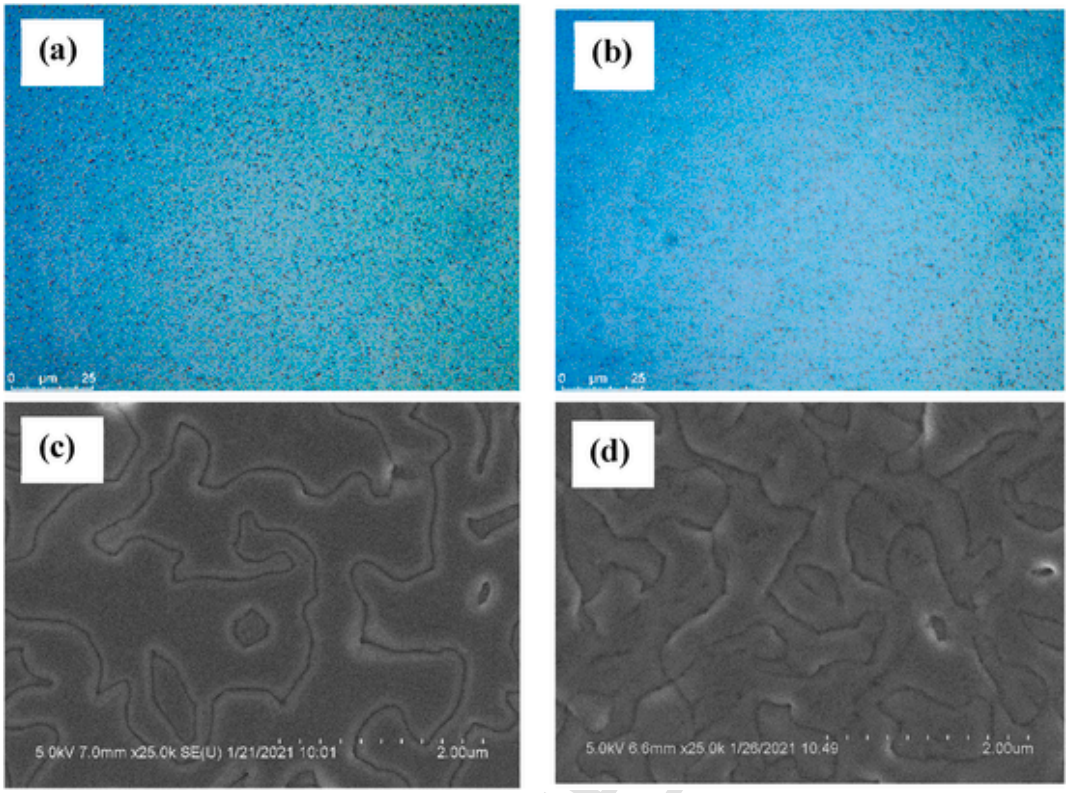

Fig. 6. Optical microscope images of the gallium arsenide film deposited by MOCVD (a) on virtual substrate and (b) on a germanium wafer. Scanning electron microscopy image of GaAs film grown by MOCVD (c) on a virtual substrate and (d) on a germanium wafer (Both silicon and germanium wafers are exactly oriented). (For interpretation of the references to colour in this figure legend, the reader is referred to the Web version of this article.)

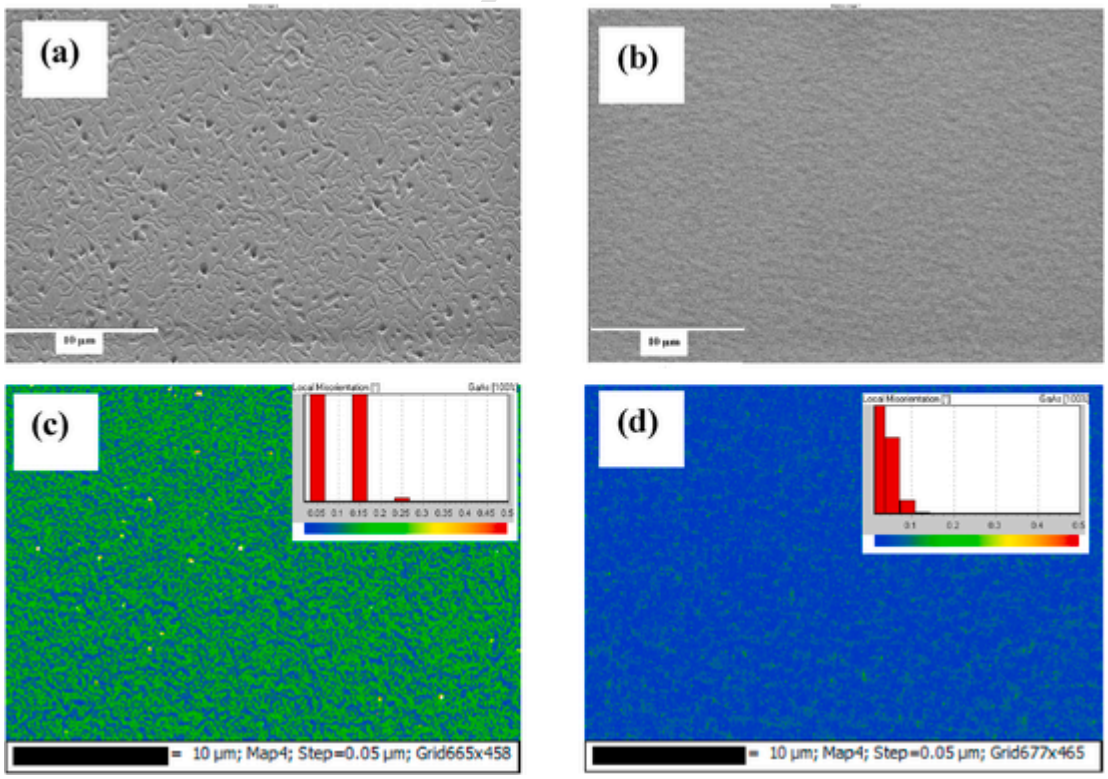

Fig. 7. Scanning electron microscopy image of GaAs deposited by MOCVD on (a) on Ge virtual substrate deposited on exactly oriented (100) c-Si wafer (Type A) and (b) Ge virtual substrate deposited on silicon wafer with 5° miscut (Type B) and EBSD analysis of GaAs samples (c) Type A and (d) Type B respectively. (For interpretation of the references to colour in this figure legend, the reader is referred to the Web version of this article.)

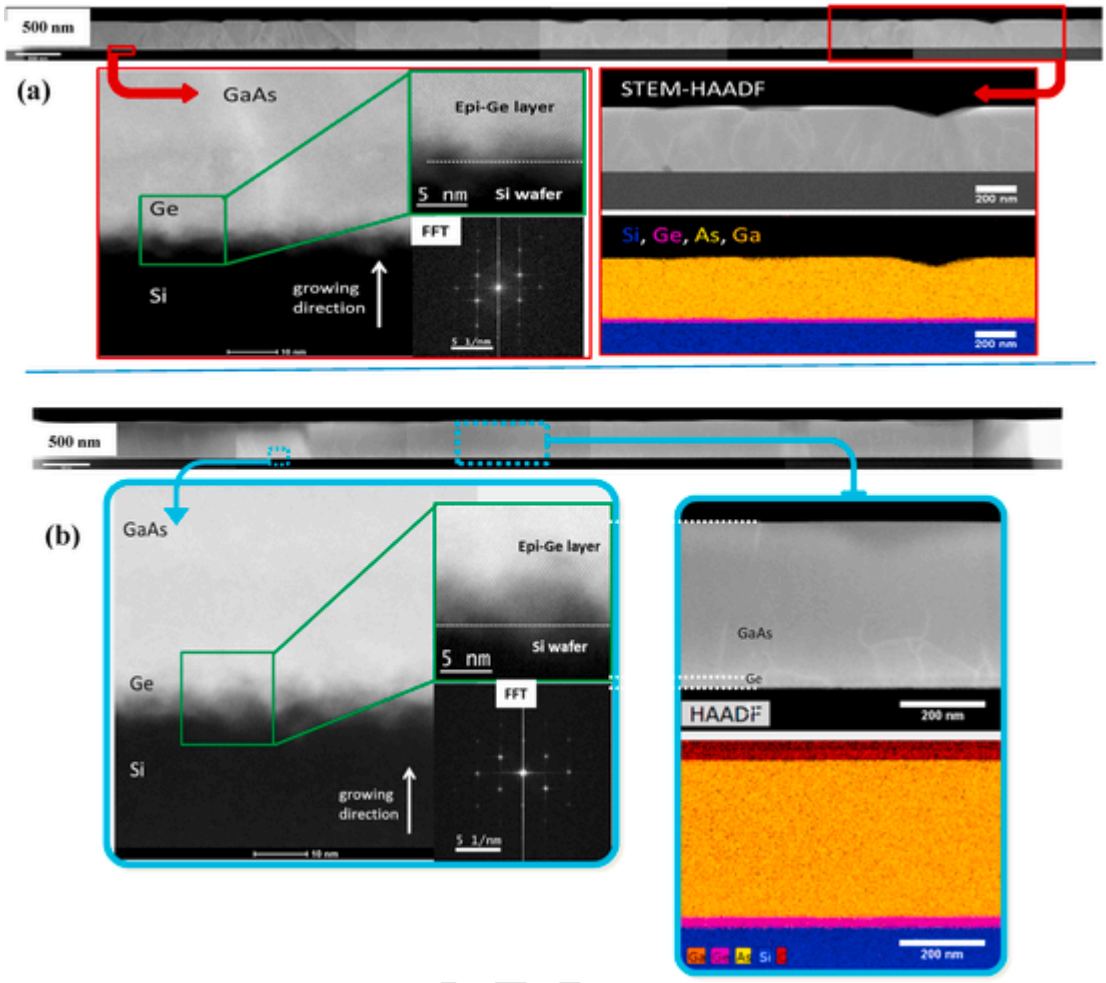

Fig. 8. HR-STEM-HAADF observations (left) and STEM-HAADF EDS chemical analysis (right) for a GaAs grown on a c-Si/c-Ge virtual substrate without miscut (type A) a) and on a 5° miscut c-Si/c-Ge virtual substrate (type B) b). For each sample the top image shows the addition of a few zones providing a large view of the cross section. The HR-STEM-HAADF observations provide a zoom on the interface with a high-resolution image in the inset and a FFT analysis demonstrating the epitaxial quality of the layers. The EDS analysis clearly show the epi-Ge layer between the c-Si substrate and the GaAs thin film.

fication and high magnification STEM-HAADF images of the corresponding lamellas. On top of each figure, we present a zone of 10 μm long representative of each sample. A detailed analysis of such images has allowed us to estimate the thickness of each layer within the samples which corresponds to 20 nm for the Ge layer and 350 nm for GaAs. Moreover, a closer analysis of all recorded images revealed the presence of threading dislocations within both samples with a density that is considerably lower (by a factor of two) for the sample of type B than the sample of type A. For type B most dislocations do not propagate within the GaAs layer from its bottom part to the surface of the film. The dislocations which travel all the GaAs layers through the surface for the type A sample can reach the domain boundaries present at the surface of the film as shown in Fig. 7 (a). The high crystallinity of both germanium and silicon at their interface can be deduced from the high-resolution STEM-HAADF images. From these images, we can also infer that the interface between the c-Si substrate and the c-Ge epitaxial film is not perfectly flat and that there is some mixing between Ge and Si atoms in a region of a few nanometers. This intermixing most likely took place during the growth of the GaAs film at high temperatures. Moreover, the corresponding STEM-HAADF EDX chemical maps obtained for both types of samples shown in Fig. 8 provide a complete image of the distribution of the principal components, Si, Ge, Ga, and As, within the two considered samples. Elemental maps were extracted at energies of 1.74 keV (Si Kα), 9.8 keV Ge (Kα), 9.24 keV Ga (Kα), 10.53 keV As (Kα).

3.2.3. GaInP/GaInAs by MOCVD

To check if the germanium films can perform equally well as a virtual substrate (20 nm Ge deposited on Silicon wafer with miscut of 5° towards <110>) for III-V materials other than GaAs, MOCVD is used to deposit a stack GaInP (200 nm)/GaInAs (500 nm) on it. On observing the film surface under scanning electron microscopy, the film appears very uniform and smooth, without antiphase boundaries or defects on the surface (Fig. 9(a)). Fig. 9 b) shows the imaginary part of the pseudo-dielectric function as deduced from ellipsometry measurements. The model of the data with the layer stack shown in the inset, allows reproducing the experimental data with the thickness of the GaInP (236 nm) and of the GaInAs layer (520 nm) a bit higher than their nominal values.

3.3. Tandem solar cell performance

GaInAs/Si tandem cell structures (see the sketch of the structure in the inset of Fig. 9 (c) are grown by MOCVD and solar cells fabricated as proof-of-concept devices. The EQE of one representative tandem solar cell is shown in Fig. 9 (d) where one can see the response of both the GaInAs and Si subcells. In this tandem, the current is obviously limited by the photocurrent in the Si bottom cell. In fact, these proof-of-concept solar cell devices are fabricated without using back surface passivation or light trapping, so the Si bottom cell spectral response has a large room for improvement. Moreover, the GaInAs top cell bandgap and

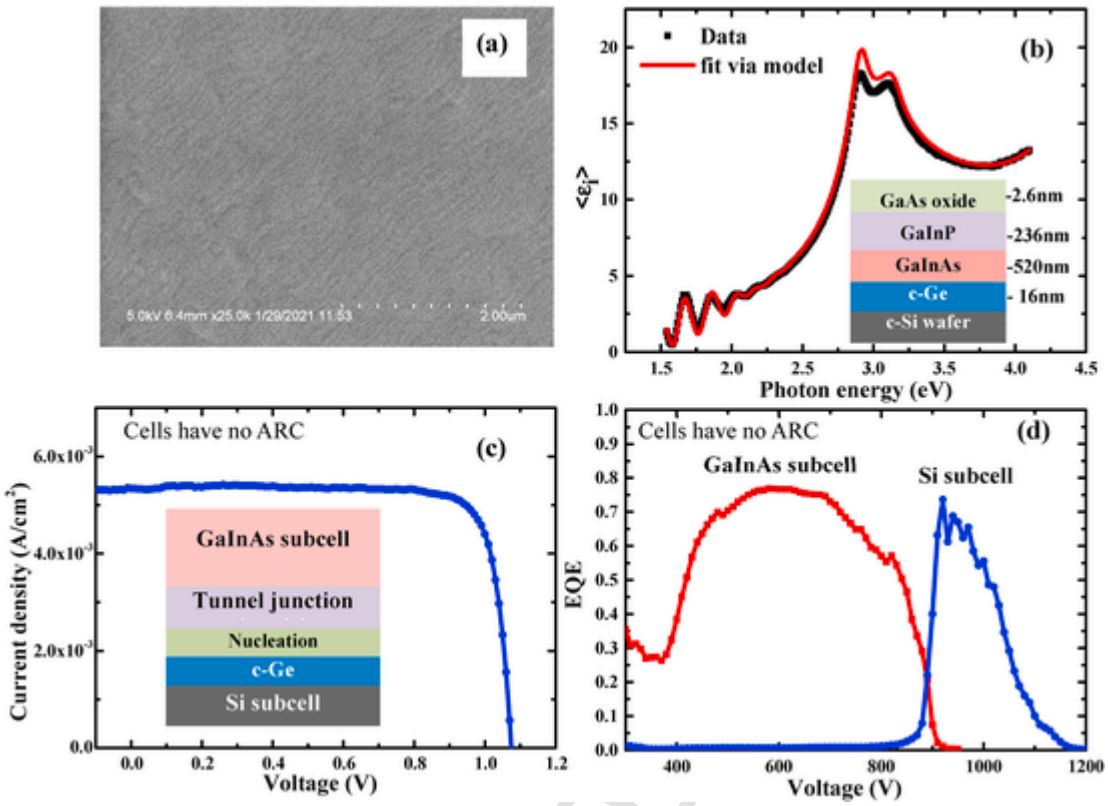

Fig. 9. (a) Scanning electron microscopy image and (b) imaginary part of the pseudo-dielectric function (inset shows the layers fitted via model)of GaInP/GaInAs films on virtual substrate. (c) J-V characteristics and (d) EQE of the devices fabricated with the GaInP/GaInAs films grown on virtual substrate by MOCVD.

thickness (2500 nm) are not suited for a current matched tandem, which would require a thinner top subcell. The EQE of the GaInAs subcell shows a lower than expected response in the low energy range of this subcell, with modeled electron diffusion lengths below 500 nm. Besides, the V_{oc} obtained from the J-V curves (~1.1 V) is also low with respect to the expected ~1.6 V GaInAs/Si stack. Further improvements in the defect density and surface morphology of the virtual substrates should drastically improve these metrics. From these data, it is clear that, beyond the current matching issue commented above, there is room for improvement in the performance of the III-V solar cells fabricated on the virtual substrates. At any rate, the light J-V and EQE curves shown in Fig. 9 (c) and (d) demonstrate proof-of-concept functional devices.

4. Summary and conclusions

In this work, we have epitaxially grown 20 nm thin layers of germanium by PECVD at 175 °C on both standard (100) crystalline silicon wafers as well as on (100) silicon wafers with a miscut of 5° towards <110>. These layers can successfully withstand high-temperature annealing in a vacuum up to 800 °C showing neither significant hydrogen desorption nor a change in their surface morphology. An *in situ* SiF_4/H_2 plasma treatment prior to the c-Ge epitaxy has been found to be the reason for such performances. The as-deposited germanium films have been used as virtual substrates for the growth of GaAs layers. Ge virtual substrates on standard (100) c-Si wafers allow the growth of GaAs epitaxially by CBE and MOCVD; however, as expected, these films have a high density of antiphase domains resulting from the growth of a polar material on a non-polar substrate. As a matter of fact, the GaAs layers deposited on flat virtual substrates have the same features as these co-deposited on a c-Ge wafer. This issue on antiphase domains has been solved by using miscut wafers. Indeed, when the germanium film is grown on a silicon wafer with miscut and in turn is used as a virtual substrate for GaAs growth by MOCVD, the surface has remained smooth and without any antiphase domains. TEM analysis has shown the presence of a far lesser number of threading dislocations for this case than virtual substrate grown on an exactly oriented (100) c-Si wafer. MOCVD was also used to successfully grow GaInP/GaInAs stacks on the virtual substrate, which opened the way to proof-of-concept tandem c-Si/GaInAs solar cells incorporating the ultrathin c-Ge layers as virtual substrate. These results demonstrate the validity of our approach and open a new perspective for low-cost tandem solar cells.

Declaration of competing interest

The authors declare that they have no known competing financial interests or personal relationships that could have appeared to influence the work reported in this paper.

Acknowledgements

The authors acknowledge financial support from the French state managed by the National Research Agency under the Investments for the Future program under the references ANR-10-EQPX-50 pole NanoMax & NanoTEM. The authors would also like to acknowledge the Centre Interdisciplinaire de Microscopie électronique de l'X (CIMEX). I. García acknowledges the financial support provided by Project ELOSIE funded by the Madrid Government (Comunidad de Madrid-Spain) under the Multiannual Agreement with Universidad Politécnica de Madrid in the line stimulation of research for young doctors, in the context of the VPRICIT (Regional Programme of Research and Technological Innovation). I. Rey-Stolle acknowledges financial support from the Spanish MCIN project RTI2018-094291-B-I00 (VIGNEMALE). The MOVPE growths at IES-UPM are part of the EQC2019-005701-P project, funded by Spanish AEI/10.13039/501100011033, the MCIN, and the ERDF "Una manera de hacer Europa".

Appendix A. Supplementary data

Supplementary data to this article can be found online at https://doi.org/10.1016/j.solmat.2021.111535.

References

[1] L.C. Bobb, H. Holloway, K.H. Maxwell, E. Zimmerman, Oriented growth of semiconductors III; growth of gallium arsenide on germanium, J. Appl. Phys. 37 (1966) 4687, https://doi.org/10.1063/1.1708118.

[2] E.K. Muller, Structure of oriented, vapor-deposited GaAs films, studied by electron diffraction, J. Appl. Phys. 35 (1964) 580, https://doi.org/10.1063/1.1713420.

[3] J. Geisz, R.M. France, K.L. Schulte, M.A. Steiner, A.G. Norman, H.L. Guthrey, M.R. Young, T. Song, T. Moriarty, Six-junction III–Vsolar cells with 47. 1% conversion efficiency under143 Suns concentration, NatureEnergy 5 (2020) 326, https://doi.org/10.1038/s41560-020-0598-5.

[4] G.J. Bauhuis, P. Mulder, E.J. Haverkamp, J.C.C.M. Huijben, J.J. Schermer, 26.1% thin-film GaAs solar cell using epitaxial lift-off, Sol. Energy Mater. Sol. Cell. 93 (2009), https://doi.org/10.1016/j.solmat.2009.03.027, 1488–149.

[5] A. van Geelen, P.R. Hageman, G.J. Bauhuis, P.C. van Rijsingen, P. Schmidt, L.J. Giling, Epitaxial lift-off GaAs solar cell from a reusable GaAs substrate, Materials Science and, Engineering. B 45 (1997) 162–171, https://doi.org/10.1016/S0921-5107(96)02029-6.

[6] K.A. Horowitz, T.W. Remo, B. Smith, A.J. Ptak, A Techno-Economic Analysis and Costreduction Roadmap for III-V Solar Cells, Technical report. National Renewable Energy Laboratory (NREL), Golden, CO (United States), 2018, NREL/TP-6A20-72103.

[7] A.B. Poungou´e Mbeunmi, M. El-Gahouchi, R. Arvinte, A. Jaouad R. Cheriton, M. Wilkins, C.E. Valdivia, K. Hinzer, S. Fafard, V. Aimez, R. Ar`es, A. Boucherie, Direct growth of GaAs solar cells on Si substrate via mesoporous Si buffer, Sol. Energy Mater. Sol. Cells 217 (2020) 110641, https://doi.org/10.1016/j.solmat.2020.110641.

[8] Y. Wang, Z. Ren, M. Thway, K. Lee, S.F. Yoon, I.M. Peters, T. Buonassisia, E.A. Fitzgerald, C.S. Tan, K.H. Lee, Fabrication and characterization of single junction GaAs solar cells on Si with As-doped Ge buffer, Sol. Energy Mater. Sol. Cell. 172 (2017) 140, https://doi.org/10.1016/j.solmat.2017.07.028.

[9] T.W. Kim, B.R. Albert, L.C. Kimerling, J. Michel, InGaP solar cell on Ge-on-Si virtual substrate for novel solar power conversion, J. Appl. Phys. 123 (2018) 085111, https://doi.org/10.1063/1.5018082.

[10] I. García, M. Hinojosa, I. Lombardero, L. Cifuentes, I. Rey-Stolle, C. Algora, H. Nguyen, S. Edwards, A. Morgan, A. Johnson, Ge Virtual Substrates for High Efficiency III-V Solar Cells: Applications, Potential and Challenges, arxiv: 1909.09499.

[11] I. García, L. Barrutia, S. Dadgostar, M. Hinojosa, A. Johnson, I. Rey-Stolle, Thinned GaInP/GaInAs/Ge solar cells grown with reduced cracking on Ge|Si virtual substrates, Sol. Energy Mater. Sol. Cells 225 (2021) 111034, https://doi.org/10.1016/j.solmat.2021.111034.

[12] H. Ye, J. Yu, Germanium epitaxy on silicon, Sci. Technol. Adv. Mater. 15 (2014) 024601, https://doi.org/10.1088/1468-6996/15/2/024601.

[13] J. Nakatsuru, H. Date, S. Mashiro, M. Ikemoto, Growth of high-quality Ge epitaxial layer on Si (100) substrate using ultra-thin Si0.5Ge0.5 buffer, Mater. Res. Soc. Symp. Proc. 891 (2006) 724, https://doi.org/10.1557/PROC-0891-EE07-24.

[14] M.T. Currie, S.B. Samavedam, T.A. Langdo, C.W. Leitz, E.A. Fitzgerald, Controlling threading dislocation densities in Ge on Si using graded SiGe layers and chemical-mechanical polishing, Appl. Phys. Lett. 72 (1998) 1718, https://doi.org/10.1063/1.121162.

[15] E.A. Fitzgerald, Y.H. Xie, M.L. Green, D. Brasen, A.R. Kortan, J. Michel, Y.J. Mii, B. E Weir, Totally relaxed GexSi1−x layers with low threading dislocation densities grown on Si substrates Appl, Phys. Lett. 59 (1991) 811, https://doi.org/10.1063/1.105351.

[16] V.A. Shah, A. Dobbie, M. Myronov, D.R. Leadley, Reverse graded SiGe/Ge/Si buffers for high-composition virtual substrates, J. Appl. Phys. 107 (2010) 064304, https://doi.org/10.1063/1.3311556.

[17] H.C. Luan, D.R. Lim, K.K. Lee, K.M. Chen, J.G. Sandland, K. Wada, L.C. Kimerling, High-quality Ge epilayers on Si with low threading-dislocation densities, Appl. Phys. Lett. 75 (1999) 2909, https://doi.org/10.1063/1.125187.

[18] Y.H. Tan, C.S. Tan, Growth and characterization of germanium epitaxial film on silicon (001) using reduced pressure chemical vapor deposition, Thin Solid Films 520 (2012) 2711, https://doi.org/10.1016/j.tsf.2011.11.046.

[19] L. Colace, G. Masini, F. Galluzzi, G. Assanto G. Capellini, L. Di Gaspare, E. Palange, F. Evangelist, Metal–semiconductor–metal near-infrared light detector based on epitaxial Ge/Si, Appl. Phys. Lett. 72 (1998) 3175, https://doi.org/10.1063/1.121584.

[20] H. Chong, Z. Wang, C. Chen, Z. Xu, K. Wu, L. Wu, B. Xu, H. Ye, Optimization of hetero-epitaxial growth for the threading dislocation density reduction of germanium epilayers, J. Cryst. Growth 488 (2018) 8–15, https://doi.org/10.1016/j.jcrysgro.2018.02.024.

[21] J.M. Hartmann, A. Abbadie, N. Cherkashin, H. Grampeix, L. Clavelier, Epitaxial growth of Ge thick layers on nominal and 6° off Si (0 0 1) Ge surface passivation by Si, Semicond. Sci. Technol. 24 (2009) 055002, https://doi.org/10.1088/0268-1242/24/5/055002.

[22] K.H. Lee, S. Bao, B. Wang, C. Wang, S. Fatt Yoon, J. Michel, E.A. Fitzgerald, C. Seng Tan, Reduction of threading dislocation density in Ge/Si using a heavily As-doped Ge seed layer, AIP Adv. 6 (2016) 025028, https://doi.org/10.1063/1.4943218.

[23] A. Ghosh, M.B. Clavel, P.D. Nguyen, M.A. Meeker, G.A. Khodaparast, R.J. Bodnar, M.K. Hudait, Growth, structural, and electrical properties of germanium-on-silicon heterostructure by molecular beam epitaxy, AIP Adv. 7 (2017) 095214, https://doi.org/10.1063/1.4993446.

[24] T.A. Langdo, C.W. Leitz, M.T. Currie, E.A. Fitzgerald, A. Lochtefeld, D.A. Antoniadis, High quality Ge on Si by epitaxial necking, Appl. Phys. Lett. 76 (2000) 3700, https://doi.org/10.1063/1.126754.

[25] J. Bai, J.-S. Park, Z. Cheng, M. Curtin, B. Adekore, M. Carroll, A. Lochtefeld, M. Dudley, Study of the defect elimination mechanisms in aspect ratio trapping Ge growth, Appl. Phys. Lett. 90 (2007) 101902, https://doi.org/10.1063/1.2711276.

[26] J. Liu, X. Sun, R. Camacho-Aguilera, L.C. Kimerling, J. Michel, Ge-on-Si laser operating at room temperature, Opt. Lett. 35 (5) (2010) 679, https://doi.org/10.1364/OL.35.000679.

[27] S. Ren, Y. Rong, T.I. Kamins, J.S. Harris, D.A.B. Miller, Selective epitaxial growth of quantum wells on Si substrate using reduced pressure chemical vapour deposition Appl, Phys. Lett. 98 (2011) 151108, https://doi.org/10.1063/1.3574912.

[28] Y. Huangfu, W. Zhan, X. Hong, X. Fang, G. Ding, H. Ye, Heteroepitaxy of Ge on Si (001) with pits and windows transferred from free-standing porous alumina mask, Nanotechnology 24 (2013) 185302, https://doi.org/10.1088/0957-4484/24/18/185302.

[29] A. Ballabio, S. Bietti, A. Scaccabarozzi, L. Esposito, S. Vichi, A. Fedorov, A. Vinattieri, C. Mannucci, F. Biccari, A. Nemcsis, L. Toth, L. Miglio, M. Gurioli, G. Isella, S. Sanguinetti, GaAs epilayers grown on patterned (001) silicon substrates via suspended Ge layers, Sci. Rep. 9 (2019) 17529, https://doi.org/10.1038/s41598-019-53949-x.

[30] M. Bollani, A. Fedorov, M. Albani, S. Bietti, R. Bergamaschini, F. Montalenti, A. Ballabio, L. Miglio, S. Sanguinetti, Selective area epitaxy of GaAs/Ge/Si nanomembranes: a morphological study, Crystals 10 (2020) 57, https://doi.org/10.3390/cryst10020057.

[31] D. Pelati, G. Patriarche, L. Largeau, O. Mauguin, L. Travers, F. Brisset, F. Glas, F. Oehler, Microstructure of GaAs thin films grown on glass using Ge seed layers fabricated by aluminium induced crystallization, Thin Solid Films 694 (2020) 137737, https://doi.org/10.1016/j.tsf.2019.137737.

[32] M. Labrune, X. Bril, G. Patriarche, L. Largeau, O. Manguin, P. Roca i Cabarrocas, Epitaxial growth of silicon and germanium on (100)-oriented crystalline substrates by RF PECVD at 175ºC, EPJ Photovoltaics 3 (2012) 30303, https://doi.org/10.1051/epjpv/2012010.

[33] R. Cariou, R. Ruggeri, X. Tan, G. Mannino, J. Nassar, P. Roca i Cabarrocas, Structural properties of relaxed thin film germanium layers grown by low temperature RF-PECVD epitaxy on Si and Ge (100) substrates, AIP Adv. 4 (2014) 077103, https://doi.org/10.1063/1.4886774.

[34] H.L.T. Le, F. Jardali, H. Vach, Deposition of hydrogenated silicon clusters for efficient epitaxial growth, Phys. Chem. Chem. Phys. 20 (2018) 15626–15634, https://doi.org/10.1039/C8CP00764K, 23.

[35] G. Hamon, N. Vaissiere, C. Lausecker, R. Cariou, W. Chen, J. Alvarez, J. L. Maurice, G. Patriarche, L. Largeau, J. Decobert, J.P. Kleider, and P. Roca i Cabarrocas, Heteroepitaxial Growth of Silicon on GaAs via Low Temperature Plasma-Enhanced Chemical Vapor Deposition, SPIE Photonics Proc. SPIE 10926, Quantum Sensing and Nano Electronics and Photonics XVI, San Francisco, 109261C (1 February 2019); DOI: 10.1117/12.2511174

[36] P. Caño, M. Hinojosa, L. Cifuentes, H. Nguyen, A. Morgan, D. Fuertes, I. García, A. Johnson, I. Rey-Stolle, Hybrid III-V/SiGe Solar Cells on Si Substrates and Porous Si Substrates, 46th. IEEE PVSC, Chicago, USA, 2019, pp. 2513–2518, https://doi.org/10.1109/PVSC40753.2019.8981138.

[37] I. García, M. Ghosh, V. Orejuela, P. Roca, I. Rey-Stolle, III-V multijunction solar cells on ultrathin Ge|Si virtual substrates grown at low temperature by RF-PECVD, Proceedings of 38th EUPVSEC (2021) 378–381, https://doi.org/10.4299/EUPVSEC20212021-3BO.10.2.

[38] P. Roca i Cabarrocas, J.B. Chévrier, J. Huc, A. Lloret, J.Y. Parey, J.P.M. Schmitt, A fully automated hot-wall multiplasma-monochamber reactor for thin film deposition, J. Vac. Sci. Technol. (1991) 2331, https://doi.org/10.1116/1.577318.

[39] M. Moreno, M. Labrune, P. Roca i Cabarrocas, Dry fabrication process for heterojunction solar cells through in-situ plasma cleaning and passivation, Sol. Energy Mater. Sol. Cell. 94 (2010) 402–405, https://doi.org/10.1016/j.solmat.2009.10.016.

[40] R. Cariou, W. Chen, J.-L. Maurice, J. Yu, G. Patriarche, O. Mauguin, L. Largeau, J. Decobert, P. Roca i Cabarrocas, Low temperature PECVD epitaxial growth of silicon on GaAs: a new paradigm for III-V/Si integration, Sci. Rep. 6 (2016) 25674, https://doi.org/10.1038/srep25674.

[41] W.T. Tsang, From chemical vapour epitaxy to chemical beam epitaxy, J. Cryst. Growth 95 (1989) 121, https://doi.org/10.1016/0022-0248(89)90364-3.

[42] J.H. Parker, D.W. Feldman, M. Ashkin, Raman scattering by silicon and germanium, Phys. Rev. 155 (1976) 712, https://doi.org/10.1103/PhysRev.155.712.

[43] R. Cariou, J. Tang, N. Ramay, R. Ruggeri, P. Roca i Cabarrocas, Low temperature epitaxial growth of SiGe absorber for thin film heterojunction solar cells, Sol. Energy Mater. Sol. Cell. 134 (2015) 15–21, https://doi.org/10.1016/j.solmat.2014.11.018.

[44] T.F. Kuech, III-V compound semiconductors: growth and structures, Prog. Cryst. Growth Char. Mater. 62 (2016) 352–370, https://doi.org/10.1016/j.pcrysgrow.2016.04.019.

[45] Q. Li, K.M. Lau, Epitaxial growth of highly mismatched III-V materials on (001) silicon for electronics and optoelectronics, Prog. Cryst. Growth Char. Mater. 63

(2017) 105, https://doi.org/10.1016/j.pcrysgrow.2017.10.00.